2021 American Control Conference (ACC)
New Orleans, USA, May 25-28, 2021

Closed-Loop Performance versus Target-Model Matching in Retrospective Cost Adaptive Control

Syed Aseem Ul Islam, Antai Xie, and Dennis S. Bernstein

***Abstract*— For retrospective cost adaptive control (RCAC), this paper shows that the retrospective performance variable can be decomposed into the sum of a performance term and a model-matching term. The key insight arises from the observation that, at each step, recursive-least-squares (RLS) minimizes the magnitude of the retrospective performance variable by forcing the performance term and the model-matching term to have opposite signs. As the controller converges, the virtual external control perturbation, and thus the model-matching term, converges to zero, which, in turn, drives the performance term to zero. This mechanism thus prevents RLS from converging to a controller that is destabilizing or has poor performance. The contribution of this paper is thus to derive the decomposition of the retrospective performance variable and use this decomposition to elucidate the mechanism described.**

I. Digital Adaptive Control

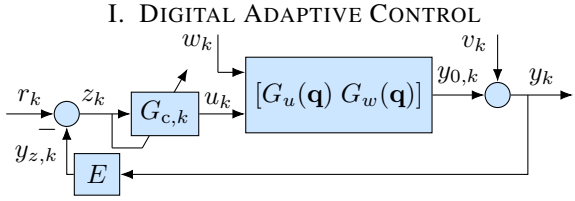

Fig. 1. Block diagram for command following and disturbance rejection under digital adaptive control.

Consider the adaptive control architecture in Figure 1, where $G_u(\mathbf{q}) \in \mathbb{R}(\mathbf{q})^{p\times m}_{\rm prop}$ and $G_w(\mathbf{q}) \in \mathbb{R}(\mathbf{q})^{p\times l}_{\rm prop}$ are proper $p \times m$ and $p \times l$ transfer functions, respectively. The plant output is $y_{0,k}$ is corrupted by sensor noise v_k to produce $y_k \in \mathbb{R}^p$. The performance variable is $y_{z,k} \triangleq Ey_k \in \mathbb{R}^q$, where the matrix $E \in \mathbb{R}^{q\times p}$ selects components of y_k or a linear combination of the components of y_k that are required to follow the command $r_k \in \mathbb{R}^q$. The command-following error is thus $z_k \triangleq r_k - y_{z,k} \in \mathbb{R}^q$, which is the input to the adaptive feedback controller $G_{c,k}(\mathbf{q})$ and serves as the adaptation variable, as denoted by the diagonal line in Figure 1 passing through $G_{c,k}(\mathbf{q})$. Note that

$$y_k = G_u(\mathbf{q})u_k + G_w(\mathbf{q})w_k + v_k, \quad z_k = r_k - Ey_k. \quad (1)$$

The adaptive feedback controller produces the control $u_k \in \mathbb{R}^m$ at each step k. The objective is to minimize the magnitude of the command-following error z_k in the presence of the disturbance w_k and sensor noise v_k.

Note that the argument $\mathbf{q}$ of G_u and G_w in (1) reflects the fact that (1) are time-domain equations whose solution depends on the initial conditions of the input-output model. The distinction between $\mathbf{z}$ and $\mathbf{q}$ in accounting for initial conditions and the resulting free response is discussed in [1], [2]. Since $G_u(\mathbf{z})$ and $G_u(\mathbf{q})$ have the same form, the argument has no effect on the algebraic properties of G_u such as poles and zeros.

Syed Aseem Ul Islam, Antai Xie, and Dennis S. Bernstein are with the Department of Aerospace Engineering, University of Michigan, Ann Arbor, MI, USA. {aseemisl, antai, dsbaero}@umich.edu

II. Retrospective Cost Adaptive Control

Consider the strictly proper dynamic compensator

$$u_k = \sum_{i=1}^{n_c} P_{i,k}u_{k-i} + \sum_{i=1}^{n_c} Q_{i,k}z_{k-i}, \quad (2)$$

where n_c is the controller window length, and $Q_{1,k},\ldots,Q_{n_c,k} \in \mathbb{R}^{m\times q}$ and $P_{1,k},\ldots,P_{n_c,k} \in \mathbb{R}^{m\times m}$ are the numerator and denominator controller coefficient matrices, respectively. The controller (2) can be written as

$$u_k = \phi_k\theta_k, \quad \phi_k \triangleq \begin{bmatrix} u_{k-1} \\ \vdots \\ u_{k-n_c} \\ z_{k-1} \\ \vdots \\ z_{k-n_c} \end{bmatrix}^{\rm T} \otimes I_m \in \mathbb{R}^{m\times l_\theta}, \quad (3)$$

where ϕ_k is the regressor, $l_\theta \triangleq n_c m(m+q)$, and the *controller coefficient vector* is defined by

$$\theta_k \triangleq \operatorname{vec}[\,P_{1,k}\ \cdots\ P_{n_c,k}\ Q_{1,k}\ \cdots\ Q_{n_c,k}\,] \in \mathbb{R}^{l_\theta}. \quad (4)$$

In terms of $\mathbf{q}$, the controller (2) can be expressed as $u_k = G_{c,k}(\mathbf{q})z_k$, where

$$N_{c,k}(\mathbf{q}) \triangleq Q_{1,k}\mathbf{q}^{n_c-1} + \cdots + Q_{n_c,k}, \quad (5)$$

$$D_{c,k}(\mathbf{q}) \triangleq I_m\mathbf{q}^{n_c} - P_{1,k}\mathbf{q}^{n_c-1} - \cdots - P_{n_c,k}, \quad (6)$$

$$G_{c,k}(\mathbf{q}) \triangleq D_{c,k}^{-1}(\mathbf{q})N_{c,k}(\mathbf{q}). \quad (7)$$

Next, in order to update the controller coefficients (4), let $\theta \in \mathbb{R}^{l_\theta}$ denote a variable for optimization, and define the filtered signals

$$u_{f,k} \triangleq G_f(\mathbf{q})u_k, \quad \phi_{f,k} \triangleq G_f(\mathbf{q})\phi_k, \quad (8)$$

where for startup, $u_{f,k}$ and $\phi_{f,k}$ are initialized at zero and thus are computed as the forced responses of (8). Unless specified otherwise, the same filter initialization is for all filters in the subsequent development. The filter $G_f(\mathbf{q})$ has the form $G_f(\mathbf{q}) \triangleq D_f(\mathbf{q})^{-1}N_f(\mathbf{q})$, where

$$N_f(\mathbf{q}) \triangleq N_{f,1}\mathbf{q}^{n_f-1} + \cdots + N_{f,n_f}, \quad (9)$$

$$D_f(\mathbf{q}) \triangleq I_m\mathbf{q}^{n_f} + D_{f,1}\mathbf{q}^{n_f-1} + \cdots + D_{f,n_f}, \quad (10)$$

n_f is the filter window length, and $N_{f,1},\ldots,N_{f,n_f} \in \mathbb{R}^{q\times m}$, and $D_{f,1},\ldots,D_{f,n_f} \in \mathbb{R}^{m\times m}$, are the numerator and denominator coefficients of $G_f(\mathbf{q})$, respectively.

Equivalently, (8) can be written as

$$u_{f,k} = NU_k - DU_{f,k}, \quad \phi_{f,k} = N\Phi_k - D\Phi_{f,k}, \quad (11)$$

where

$$U_k \triangleq \begin{bmatrix} u_{k-1} \\ \vdots \\ u_{k-n_\mathrm{f}} \end{bmatrix} \in \mathbb{R}^{n_\mathrm{f} m}, \quad U_{\mathrm{f},k} \triangleq \begin{bmatrix} u_{\mathrm{f},k-1} \\ \vdots \\ u_{\mathrm{f},k-n_\mathrm{f}} \end{bmatrix} \in \mathbb{R}^{n_\mathrm{f} m}, \tag{12}$$

$$\Phi_k \triangleq \begin{bmatrix} \phi_{k-1} \\ \vdots \\ \phi_{k-n_\mathrm{f}} \end{bmatrix} \in \mathbb{R}^{n_\mathrm{f} m \times l_\theta}, \Phi_{\mathrm{f},k} \triangleq \begin{bmatrix} \phi_{\mathrm{f},k-1} \\ \vdots \\ \phi_{\mathrm{f},k-n_\mathrm{f}} \end{bmatrix} \in \mathbb{R}^{n_\mathrm{f} m \times l_\theta}, \tag{13}$$

$$N \triangleq [\, N_{\mathrm{f},1} \cdots N_{\mathrm{f},n_\mathrm{f}} \,] \in \mathbb{R}^{q \times m n_\mathrm{f}}, \tag{14}$$

$$D \triangleq [\, D_{\mathrm{f},1} \cdots D_{\mathrm{f},n_\mathrm{f}} \,] \in \mathbb{R}^{m \times m n_\mathrm{f}}. \tag{15}$$

Next, in order to update the controller coefficient vector θ, define the *retrospective performance variable*

$$\hat{z}_k(\theta) \triangleq z_k - (u_{\mathrm{f},k} - \phi_{\mathrm{f},k}\theta), \tag{16}$$

where z_k is given by (1). Note that $u_{\mathrm{f},k}$ depends on u_k and thus on the current controller coefficient vector θ_k. The retrospective performance variable $\hat{z}_k(\theta)$ is used to determine the updated controller coefficient vector θ_{k+1} by minimizing a function of $\hat{z}_k(\theta)$. The optimized value of $\hat{z}_k$ is given by

$$\hat{z}_k(\theta_{k+1}) = z_k - (u_{\mathrm{f},k} - \phi_{\mathrm{f},k}\theta_{k+1}), \tag{17}$$

which shows that the updated controller coefficient vector θ_{k+1} is "applied" retrospectively with the filtered controller regressor $\phi_{\mathrm{f},k}$. Note that the filter $G_\mathrm{f}(\mathbf{q})$ is used to obtain $\phi_{\mathrm{f},k}$ from ϕ_k by means of (8) but ignores past changes in the controller coefficient vector, as can be seen by the product $\phi_{\mathrm{f},k}\theta_{k+1}$ in (17). Consequently, the filtering used to construct (17) ignores changes in the controller coefficient vector over the window $[k - n_\mathrm{f}, k]$. The effect of the actual time-dependence of θ_k is analyzed in later sections.

In order to account for control effort, we define

$$z_{\mathrm{c},k}(\theta) \triangleq \begin{bmatrix} E_z \hat{z}_k(\theta) \\ E_u \phi_k \theta \end{bmatrix} \in \mathbb{R}^{q+r}, \tag{18}$$

where the performance weighting $E_z \in \mathbb{R}^{q \times q}$ is nonsingular, and $E_u \in \mathbb{R}^{r \times m}$ is the control weighting. If $E_u = 0$, then we set $r = 0$ and omit all expressions involving E_u in (18) as well as in all subsequent expressions. Using (16), it follows that (18) can be expressed as

$$z_{\mathrm{c},k}(\theta) = y_{\mathrm{c},k} - \phi_{\mathrm{c},k}\theta, \tag{19}$$

$$y_{\mathrm{c},k} \triangleq \begin{bmatrix} E_z z_k - E_z u_{\mathrm{f},k} \\ 0_{r \times 1} \end{bmatrix} \in \mathbb{R}^{q+r}, \tag{20}$$

$$\phi_{\mathrm{c},k} \triangleq \begin{bmatrix} -E_z \phi_{\mathrm{f},k} \\ -E_u \phi_k \end{bmatrix} \in \mathbb{R}^{(q+r) \times l_\theta}. \tag{21}$$

Using (18), we define the *retrospective cost*

$$J_k(\theta) \triangleq \sum_{i=0}^{k} z_{\mathrm{c},i}(\theta)^\mathrm{T} z_{\mathrm{c},i}(\theta) + (\theta - \theta_0)^\mathrm{T} P_0^{-1} (\theta - \theta_0). \tag{22}$$

For all $k \geq 0$, the minimizer θ_{k+1} of (22) is given by the recursive least squares (RLS) solution [3]

$$P_{k+1} = P_k - P_k \phi_{\mathrm{c},k}^\mathrm{T} (I_{q+r} + \phi_{\mathrm{c},k} P_k \phi_{\mathrm{c},k}^\mathrm{T})^{-1} \phi_{\mathrm{c},k} P_k, \tag{23}$$

$$\theta_{k+1} = \theta_k + P_{k+1} \phi_{\mathrm{c},k}^\mathrm{T} (y_{\mathrm{c},k} - \phi_{\mathrm{c},k}\theta_k). \tag{24}$$

Using the updated controller coefficients given by (24), the requested control input at step $k+1$ is given by $u_{k+1} = \phi_{k+1}\theta_{k+1}$. Although θ_0 can be chosen arbitrarily, we choose $\theta_0 = 0$ to reflect the absence of additional modeling information, and we set $P_0 = p_0 I_{l_\theta}$ where $p_0 \in (0, \infty)$ is a tuning hyperparameter.

III. Decomposition of $\hat{z}_k(\theta_{k+1})$

This section shows that $\hat{z}_k(\theta_{k+1})$ can be decomposed into the sum of a performance term and a model-matching term. We assume that the RLS update law (23), (24) is used to advance the controller coefficients θ_k to θ_{k+1}.

Since the optimized controller coefficient vector is time-dependent, $\hat{z}_k(\theta)$ defined by (16) must be modified to ignore the time-dependence of θ_{k+1}. To do this, the terms $u_{\mathrm{f},k} - \phi_{\mathrm{f},k}\theta$ in (16) are replaced by a filtered version of $u_k - \phi_k\theta$ in which the controller coefficient vector is constrained to be θ_{k+1} over the filtering window. By defining

$$\tilde{u}_k(\theta_\mathrm{c}) \triangleq u_k - \phi_k \theta, \tag{25}$$

the filtered signal $\tilde{u}_{\mathrm{f},k}(\theta_{k+1})$ is given by a fixed-input-argument (FIA) filter with input $\tilde{u}_k(\theta_{k+1})$. In particular, $\tilde{u}_{\mathrm{f},k}(\theta_{k+1})$ is defined to be the output of the FIA filter

$$\tilde{u}_{\mathrm{f},k}(\theta_{k+1}) \triangleq G_\mathrm{f}(\mathbf{q}) \tilde{u}_k(\theta_{\overline{k+1}}), \tag{26}$$

which ignores the change in the argument θ_{k+1} of $\tilde{u}_k$ over the interval $[k - n_\mathrm{f}, k]$ in accordance with retrospective optimization. Note that, by the definition of FIA filtering, the filtered signal $\tilde{u}_{\mathrm{f},k}(\theta_{k+1})$ is a function of the time-dependent controller coefficient vector θ_{k+1}. The FIA filter (26) is implemented as

$$\tilde{u}_{\mathrm{f},k}(\theta_{\mathrm{c},k+1}) = -D\widetilde{U}_{\mathrm{f},k} + N\widetilde{U}_k(\theta_{\mathrm{c},k+1}), \tag{27}$$

$$\widetilde{U}_k(\theta) \triangleq \begin{bmatrix} \tilde{u}_{k-1}(\theta) \\ \vdots \\ \tilde{u}_{k-n_\mathrm{f}}(\theta) \end{bmatrix} \in \mathbb{R}^{n_\mathrm{f} m}, \tag{28}$$

$$\widetilde{U}_{\mathrm{f},k} \triangleq \begin{bmatrix} \tilde{u}_{\mathrm{f},k-1}(\theta_k) \\ \vdots \\ \tilde{u}_{\mathrm{f},k-n_\mathrm{f}}(\theta_{k-n_\mathrm{f}+1}) \end{bmatrix} \in \mathbb{R}^{n_\mathrm{f} q}, \tag{29}$$

Using (26), the definition (16) of $\hat{z}_k(\theta)$ is replaced by

$$\hat{z}_{\mathrm{ext},k}(\theta_{k+1}) \triangleq z_k - \tilde{u}_{\mathrm{f},k}(\theta_{k+1}). \tag{30}$$

Note that, if, for all k, $\theta_{k+1} = \theta$, or $G_\mathrm{f}(\mathbf{q})$ is FIR, then $\hat{z}_{\mathrm{ext},k}(\theta_{k+1}) = \hat{z}_k(\theta)$.

The following result presents the *retrospective performance-variable decomposition*, which shows that $\hat{z}_{\mathrm{ext},k}(\theta_{k+1})$ is a combination of the closed-loop performance and the extent to which the updated closed-loop transfer function from $\tilde{u}_k(\theta_{k+1})$ to z_k matches the filter $G_\mathrm{f}(\mathbf{q})$. Henceforth, we call $G_\mathrm{f}(\mathbf{q})$ the *target model*, since it serves as the target for the closed-loop transfer function from $\tilde{u}_k(\theta_{k+1})$ to z_k.

Proposition 1: Assume that $G_u(\mathbf{q})$ and $G_w(\mathbf{q})$ are strictly proper. Then, for all $k \geq 0$,

$$\hat{z}_{\mathrm{ext},k}(\theta_{k+1}) = z_{\mathrm{opp},k}(\theta_{k+1}) + z_{\mathrm{tmp},k}(\theta_{k+1}), \tag{31}$$

where the *one-step predicted performance* $z_{\mathrm{opp},k}(\theta_{k+1})$ and the *target-model matching performance* $z_{\mathrm{tmp},k}(\theta_{k+1})$ are defined by

$$z_{\mathrm{opp},k}(\theta_{k+1}) \triangleq \widetilde{G}_{zw,k+1}(\mathbf{q})[r_k - Ev_k - EG_w(\mathbf{q})w_k], \tag{32}$$

$$z_{\mathrm{tmp},k}(\theta_{k+1}) \triangleq [\widetilde{G}_{z\tilde{u},k+1}(\mathbf{q}) - G_\mathrm{f}(\mathbf{q})]\tilde{u}_k(\theta_{\overline{k+1}}), \tag{33}$$

and

$$\widetilde{G}_{zw,k+1}(\mathbf{q}) \triangleq [I_q + EG_u(\mathbf{q})G_{\mathrm{c},k+1}(\mathbf{q})]^{-1}, \quad (34)$$

$$\widetilde{G}_{z\tilde{u},k+1}(\mathbf{q}) \triangleq -\mathbf{q}^{n_\mathrm{c}}[I_q + EG_u(\mathbf{q})G_{\mathrm{c},k+1}(\mathbf{q})]^{-1} \cdot EG_u(\mathbf{q})D_{\mathrm{c},k+1}^{-1}(\mathbf{q}). \quad (35)$$

Proof. It follows from (32) and (34) that

$$z_{\mathrm{opp},k}(\theta_{k+1}) = r_k - Ev_k - EG_w(\mathbf{q})w_k - EG_u(\mathbf{q})G_{\mathrm{c},k+1}(\mathbf{q})z_{\mathrm{opp},k}(\theta_{k+1}). \quad (36)$$

Furthermore, defining the FIA filter output

$$\tilde{z}_{\mathrm{tmp},k}(\theta_{k+1}) \triangleq \widetilde{G}_{z\tilde{u},k+1}(\mathbf{q})\tilde{u}_k(\theta_{\overline{k+1}}), \quad (37)$$

it follows from (35) and (37) that

$$\tilde{z}_{\mathrm{tmp},k}(\theta_{k+1}) = -EG_u(\mathbf{q})D_{\mathrm{c},k+1}^{-1}(\mathbf{q})\mathbf{q}^{n_\mathrm{c}}\tilde{u}_k(\theta_{\overline{k+1}}) - EG_u(\mathbf{q})G_{\mathrm{c},k+1}(\mathbf{q})\tilde{z}_{\mathrm{tmp},k}(\theta_{k+1}). \quad (38)$$

Now, replacing $\mathbf{q}^{n_\mathrm{c}}\tilde{u}_k(\theta_{\overline{k+1}})$ with $\tilde{u}_{k+n_\mathrm{c}}(\theta_{k+1})$ in (38) yields

$$\tilde{z}_{\mathrm{tmp},k}(\theta_{k+1}) = -EG_u(\mathbf{q})D_{\mathrm{c},k+1}^{-1}(\mathbf{q})\tilde{u}_{k+n_\mathrm{c}}(\theta_{k+1}) - EG_u(\mathbf{q})G_{\mathrm{c},k+1}(\mathbf{q})\tilde{z}_{\mathrm{tmp},k}(\theta_{k+1}). \quad (39)$$

Combining (36) and (37) yields

$$z_{\mathrm{opp},k}(\theta_{k+1}) + \tilde{z}_{\mathrm{tmp},k}(\theta_{k+1}) = r_k - Ev_k - EG_w(\mathbf{q})w_k - EG_u(\mathbf{q})D_{\mathrm{c},k+1}^{-1}(\mathbf{q})\tilde{u}_{k+n_\mathrm{c}}(\theta_{k+1}) - EG_u(\mathbf{q})G_{\mathrm{c},k+1}(\mathbf{q}) \cdot[z_{\mathrm{opp},k}(\theta_{k+1}) + \tilde{z}_{\mathrm{tmp},k}(\theta_{k+1})]. \quad (40)$$

Replacing k with $k+n_\mathrm{c}$ in (25) and setting $\theta = \theta_{k+1}$ yields

$$\tilde{u}_{k+n_\mathrm{c}}(\theta_{k+1}) = u_{k+n_\mathrm{c}} - \phi_{\mathrm{c},k+n_\mathrm{c}}\theta_{k+1}. \quad (41)$$

Hence, using

$$\phi_{k+n_\mathrm{c}}\theta_{k+1} = \sum_{i=1}^{n_\mathrm{c}} P_{i,k+1}u_{k+n_\mathrm{c}-i} + \sum_{i=1}^{n_\mathrm{c}} Q_{i,k+1}z_{k+n_\mathrm{c}-i},$$

(5), and (6), it follows that (41) can be written as

$$\tilde{u}_{k+n_\mathrm{c}}(\theta_{k+1}) = D_{\mathrm{c},k+1}(\mathbf{q})u_k - N_{\mathrm{c},k+1}(\mathbf{q})z_k,$$

which can be combined with (40) to obtain

$$z_{\mathrm{opp},k}(\theta_{k+1}) + \tilde{z}_{\mathrm{tmp},k}(\theta_{k+1}) = r_k - Ev_k - EG_w(\mathbf{q})w_k - EG_u(\mathbf{q})u_k + EG_u(\mathbf{q})G_{\mathrm{c},k+1}(\mathbf{q})z_k - EG_u(\mathbf{q})G_{\mathrm{c},k+1}(\mathbf{q})[z_{\mathrm{opp},k}(\theta_{k+1}) + \tilde{z}_{\mathrm{tmp},k}(\theta_{k+1})]. \quad (42)$$

Using (1), it follows from (42) that

$$(I_q + EG_u(\mathbf{q})G_{\mathrm{c},k+1}(\mathbf{q}))[z_{\mathrm{opp},k}(\theta_{k+1}) + \tilde{z}_{\mathrm{tmp},k}(\theta_{k+1})] = (I_q + EG_u(\mathbf{q})G_{\mathrm{c},k+1}(\mathbf{q}))z_k, \quad (43)$$

which implies that

$$z_k = z_{\mathrm{opp},k}(\theta_{k+1}) + \tilde{z}_{\mathrm{tmp},k}(\theta_{k+1}). \quad (44)$$

Next, substituting (44) into (30) yields

$$\hat{z}_{\mathrm{ext},k}(\theta_{k+1}) = z_{\mathrm{opp},k}(\theta_{k+1}) + \tilde{z}_{\mathrm{tmp},k}(\theta_{k+1}) - \tilde{u}_{\mathrm{f},k}(\theta_{k+1}). \quad (45)$$

Hence, substituting (26) and (37) into (45) and using (33) yields

$$\begin{aligned}\hat{z}_{\mathrm{ext},k}(\theta_{k+1}) &= z_{\mathrm{opp},k}(\theta_{k+1}) + \widetilde{G}_{z\tilde{u},k+1}(\mathbf{q})\tilde{u}_k(\theta_{\overline{k+1}}) - G_\mathrm{f}(\mathbf{q})\tilde{u}_k(\theta_{\overline{k+1}}) \\ &= z_{\mathrm{opp},k}(\theta_{k+1}) + [\widetilde{G}_{z\tilde{u},k+1}(\mathbf{q}) - G_\mathrm{f}(\mathbf{q})]\tilde{u}_k(\theta_{\overline{k+1}}) \\ &= z_{\mathrm{opp},k}(\theta_{k+1}) + z_{\mathrm{tmp},k}(\theta_{k+1}). \qquad \square\end{aligned}$$

In the case where z_k, y_k, and u_k are scalar, that is, $q = p = m = 1$, (34) and (35) have the form

$$\widetilde{G}_{zw,k}(\mathbf{q}) = \frac{D_u(\mathbf{q})D_{\mathrm{c},k}(\mathbf{q})}{D_u(\mathbf{q})D_{\mathrm{c},k}(\mathbf{q}) + EN_u(\mathbf{q})N_{\mathrm{c},k}(\mathbf{q})}, \quad (46)$$

$$\widetilde{G}_{z\tilde{u},k}(\mathbf{q}) = \frac{-\mathbf{q}^{n_\mathrm{c}}EN_u(\mathbf{q})}{D_u(\mathbf{q})D_{\mathrm{c},k}(\mathbf{q}) + EN_u(\mathbf{q})N_{\mathrm{c},k}(\mathbf{q})}, \quad (47)$$

where $G_u(\mathbf{q}) \triangleq \frac{N_u(\mathbf{q})}{D_u(\mathbf{q})}$.

A. Analysis of the $\hat{z}_{\mathrm{ext},k}(\theta_{k+1})$ Decomposition

Assuming $E_z = I$, $E_u = 0$, and using (18), it follows from (22) that

$$J_k(\theta_{k+1}) = \sum_{i=0}^{k} \hat{z}_i^{\mathrm{T}}(\theta_{i+1})\hat{z}_{,i}(\theta_{i+1}) + (\theta_{i+1} - \theta_0)^{\mathrm{T}}P_0^{-1}(\theta_{i+1} - \theta_0). \quad (48)$$

In the case where p_0 is large, minimization using RLS yields $\hat{z}_k(\theta_{k+1}) \approx 0$. Furthermore, it is observed numerically and shown in Figure 3 that using RLS to minimize (48) yields $\hat{z}_{\mathrm{ext},k}(\theta_{k+1}) \approx \hat{z}_k(\theta_{k+1})$, which, using (31), implies that $z_{\mathrm{opp},k}(\theta_{k+1}) + z_{\mathrm{tmp},k}(\theta_{k+1}) \approx 0$, that is,

$$z_{\mathrm{opp},k}(\theta_{k+1}) \approx -z_{\mathrm{tmp},k}(\theta_{k+1}). \quad (49)$$

The following example illustrates this property.

Example 1. *Illustration of the $\hat{z}_{\mathrm{ext},k}(\theta_{k+1})$ decomposition.* Let

$$G_u(\mathbf{q}) = G_w(\mathbf{q}) = \frac{(\mathbf{q} - 1.1)(\mathbf{q} - 0.9)}{(\mathbf{q} - 0.85)(\mathbf{q}^2 - 1.9\mathbf{q} + 0.95)}, \quad (50)$$

and w_k and v_k be white, zero-mean Gaussian sequences with standard deviations 0.1 and 0.01, respectively. For $r_k = 0$, RCAC is applied with $E_z = 1$, $E_u = 0$, $E = 1$, $G_\mathrm{f}(\mathbf{q}) = \frac{-(\mathbf{q}-1.1)}{\mathbf{q}^2}$, $n_\mathrm{c} = 16$, and $p_0 = 10$. Figures 2(f) and 2(h) show that, for $5 \le k \le 125$, $|z_{\mathrm{opp},k}(\theta_{k+1})|$ and $|z_{\mathrm{tmp},k}(\theta_{k+1})|$ have large magnitudes, have opposite signs, and approximately sum to zero. Figure 2(g) shows that $\widetilde{G}_{z\tilde{u},500}(\mathbf{q})$ and $G_\mathrm{f}(\mathbf{q})$ have similar frequency responses, and thus the controller update promotes matching between the closed-loop transfer function $\widetilde{G}_{z\tilde{u},k+1}(\mathbf{q})$ and the target model $G_\mathrm{f}(\mathbf{q})$.

Next, in order to compare $\hat{z}_k(\theta_{k+1})$ and $\hat{z}_{\mathrm{ext},k}(\theta_{k+1})$ for the case where $G_\mathrm{f}(\mathbf{q})$ is IIR, the simulation is repeated with $G_\mathrm{f}(\mathbf{q}) = -\frac{(\mathbf{q}-1.1)}{\mathbf{q}^2+0.1\mathbf{q}+0.01}$. Figure 3 shows that the error between $\hat{z}_k(\theta_{k+1})$ and $\hat{z}_{\mathrm{ext},k(\theta_{k+1})}$ is less than 10^{-2} for all k. $\diamond$

Proposition 2: Assume that $\overline{\theta} \triangleq \lim_{k\to\infty} \theta_{k+1}$ exists and ϕ_{k+1} is bounded. Then $\lim_{k\to\infty} \tilde{u}_k(\theta_{k+1}) = 0$.

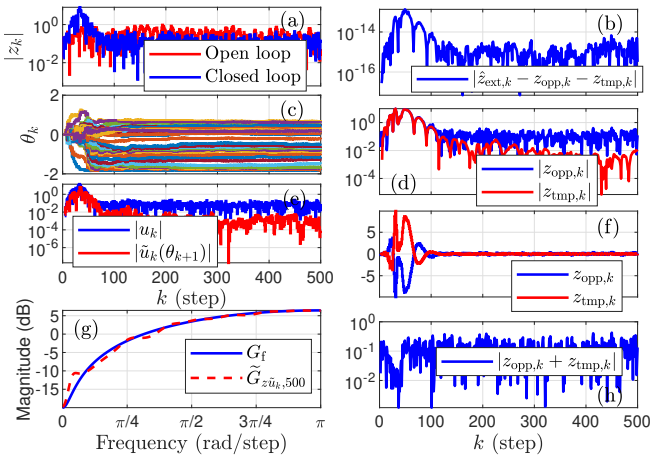

Fig. 2. Example 1: (a) open- and closed-loop responses; (b) $|\hat{z}_{\mathrm{ext},k} - z_{\mathrm{opp},k} - z_{\mathrm{tmp},k}| < 10^{-13}$ for all t, confirming (31).

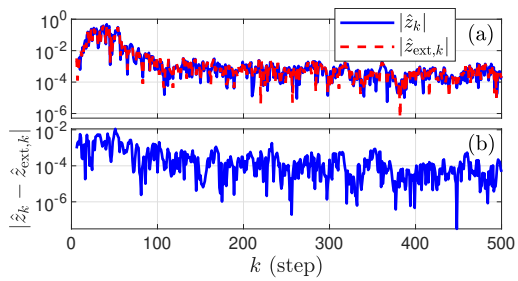

Fig. 3. Example 1: For an IIR $G_{\mathrm{f}}(\mathbf{q})$, (a) shows the absolute value of the retrospective cost variable and its extension, and (b) shows the absolute error between the retrospective cost variable and its extension.

Proof. Equations (3) and (25) imply that

$$\tilde{u}_k(\theta_{k+1}) = \phi_k(\theta_k - \theta_{k+1}).$$

Defining $\alpha = \sup_{k\geq 0} \sigma_{\max}(\phi_k)$, it follows that

$$\|\tilde{u}_k(\theta_{k+1})\| \leq \sigma_{\max}(\phi_k)\|\theta_k - \theta_{k+1}\| \quad \leq \alpha\|\theta_k - \theta_{k+1}\|,$$

where $\sigma_{\max}$ denotes the maximum singular value. Hence,

$$\lim_{k\to\infty} \|\tilde{u}_k(\theta_{k+1})\| \leq \alpha \lim_{k\to\infty} \|\theta_k - \theta_{k+1}\| = 0. \qquad \square$$

Proposition 2 suggests that the convergence of θ_k implies that $z_{\mathrm{tmp},k}(\theta_{k+1})$ converges to zero, as observed in Figure 2(f). Therefore, it follows from (49) that $|z_{\mathrm{opp},k}(\bar{\theta})| \approx 0$, and θ_k converges only if $|z_{\mathrm{opp},k}(\bar{\theta})|$ is small. This mechanism underlies the convergence of RCAC in Figure 2 to a stabilizing controller that rejects the unknown disturbance.

B. Feasibility of $G_{\mathrm{f}}(\mathbf{q})$

The following definition concerns the case where there exists a controller parameter vector that exactly matches the transfer function from $\tilde{u}_k(\theta_{k+1})$ to z_k to $G_{\mathrm{f}}(\mathbf{q})$.

Definition 1: $G_{\mathrm{f}}(\mathbf{q}) \in \mathbb{R}(\mathbf{q})^{q\times m}_{\mathrm{prop}}$ is feasible if there exists $\theta = \mathrm{vec}\,[\,P_1 \cdots P_{n_{\mathrm{c}}}\; Q_1 \cdots Q_{n_{\mathrm{c}}}\,] \in \mathbb{R}^{l_\theta}$ such that $\widetilde{G}_{z\tilde{u}}(\mathbf{q}) = G_{\mathrm{f}}(\mathbf{q})$, where

$$\widetilde{G}_{z\tilde{u}}(\mathbf{q}) \triangleq -\mathbf{q}^{n_{\mathrm{c}}}[I_q + EG_u(\mathbf{q})G_{\mathrm{c}}(\mathbf{q})]^{-1}EG_u(\mathbf{q})D_{\mathrm{c}}(\mathbf{q})^{-1}, \tag{51}$$

$$N_{\mathrm{c}}(\mathbf{q}) \triangleq Q_1\mathbf{q}^{n_{\mathrm{c}}-1} + \cdots + Q_{n_{\mathrm{c}}}, \tag{52}$$

$$D_{\mathrm{c}}(\mathbf{q}) \triangleq I_m\mathbf{q}^{n_{\mathrm{c}}} - P_1\mathbf{q}^{n_{\mathrm{c}}-1} - \cdots - P_{n_{\mathrm{c}}}, \tag{53}$$

$$G_{\mathrm{c}}(\mathbf{q}) \triangleq D_{\mathrm{c}}^{-1}(\mathbf{q})N_{\mathrm{c}}(\mathbf{q}). \tag{54}$$

If $\lim_{k\to\infty} \widetilde{G}_{z\tilde{u},k}(\mathbf{q})$ exists, then the asymptotic feasibility distance is defined by

$$\mathrm{f}_\infty \triangleq \|\lim_{k\to\infty} \widetilde{G}_{z\tilde{u},k}(\mathbf{q}) - G_{\mathrm{f}}(\mathbf{q})\|_\infty. \tag{55}$$

For the SISO case, the following result identifies various features of $\widetilde{G}_{z\tilde{u}}(\mathbf{q})$ that are determined by $G_u(\mathbf{q})$.

Proposition 3: For all $k \geq 0$, assume that $z_k, y_k, u_k \in \mathbb{R}$. Furthermore, let $\theta \in \mathbb{R}^{l_\theta}$ and $G_{\mathrm{f}}(\mathbf{q}) \in \mathbb{R}(\mathbf{q})_{\mathrm{prop}}$. Then the following statements hold:

i) The leading numerator coefficient of $\widetilde{G}_{z\tilde{u}}(\mathbf{q})$ is equal to the leading numerator coefficient of $-EG_u(\mathbf{q})$.

ii) The relative degree of $\widetilde{G}_{z\tilde{u}}(\mathbf{q})$ is equal to the relative degree of $G_u(\mathbf{q})$.

iii) The zeros of $\widetilde{G}_{z\tilde{u}}(\mathbf{q})$ consist of the zeros of $G_u(\mathbf{q})$ as well as n_{c} zeros at zero.

Proof. Since z_k and u_k are scalar, it follows that E is scalar and (51) specializes to

$$\widetilde{G}_{z\tilde{u}}(\mathbf{q}) = \frac{-\mathbf{q}^{n_{\mathrm{c}}}EN_u(\mathbf{q})}{D_u(\mathbf{q})D_{\mathrm{c}}(\mathbf{q}) + EN_u(\mathbf{q})N_{\mathrm{c}}(\mathbf{q})}, \tag{56}$$

which implies *i)*. To prove *ii)*, let n_{d} denote the degree of $D_u(\mathbf{q})$, and let $r_{\mathrm{d}} \geq 0$ denote the relative degree of $G_u(\mathbf{q})$, so that the degree of $N_u(\mathbf{q})$ is $n_{\mathrm{d}} - r_{\mathrm{d}}$. Since the degrees of $\mathbf{q}^{n_{\mathrm{c}}}EN_u(\mathbf{q})$ and $D_u(\mathbf{q})D_{\mathrm{c}}(\mathbf{q}) + EN_u(\mathbf{q})N_{\mathrm{c}}(\mathbf{q})$ are $n_{\mathrm{c}} + n_{\mathrm{d}} - r_{\mathrm{d}}$ and $n_{\mathrm{c}} + n_{\mathrm{d}}$, respectively, it follows that the relative degree of $\widetilde{G}_{z\tilde{u}}(\mathbf{q})$ is r_{d}. *iii)* follows from the fact that the numerator of (56) is the numerator of $\mathbf{q}^{n_{\mathrm{c}}}EG_u(\mathbf{q})$. $\square$

The following result, which is an immediate consequence of Proposition 3, provides necessary conditions for feasibility in the SISO case.

Proposition 4: For all $k \geq 0$, assume that $z_k, y_k, u_k \in \mathbb{R}$. Furthermore, let $\theta \in \mathbb{R}^{l_\theta}$, let $G_{\mathrm{f}}(\mathbf{q}) \in \mathbb{R}(\mathbf{q})_{\mathrm{prop}}$, and assume that $G_{\mathrm{f}}(\mathbf{q})$ is feasible. Then the following statements hold:

i) The leading numerator coefficient of $G_{\mathrm{f}}(\mathbf{q})$ is equal to the leading numerator coefficient of $-EG_u(\mathbf{q})$.

ii) The relative degree of $G_{\mathrm{f}}(\mathbf{q})$ is equal to the relative degree of $G_u(\mathbf{q})$.

iii) The zeros of $G_{\mathrm{f}}(\mathbf{q})$ consist of the zeros of $G_u(\mathbf{q})$ as well as n_{c} zeros at zero.

C. RCAC with Feasible and Infeasible $G_{\mathrm{f}}(\mathbf{q})$

For all of the examples in this subsection, let w_k and v_k be white, zero-mean Gaussian sequences with standard deviations 0.1 and 0.01, respectively. For $r_k = 0$, RCAC is applied with $E_z = 1$, $E_u = 0$, $E = 1$, and $n_{\mathrm{c}} = n$ for various choices of the target model $G_{\mathrm{f}}(\mathbf{q})$.

An LQG controller $G_{\mathrm{c,LQG}}(\mathbf{q})$ is designed for $G_u(\mathbf{q})$ using the MATLAB command lqg with $Q_{xu} = Q_{wv} = I_4$. Using (56) and the LQG controller yields

$$G_{\mathrm{f,LQG}}(\mathbf{q}) = \frac{-\mathbf{q}^{n}N_u(\mathbf{q})}{D_u(\mathbf{q})D_{\mathrm{LQG}}(\mathbf{q}) + N_u(\mathbf{q})N_{\mathrm{LQG}}(\mathbf{q})}, \tag{57}$$

where $G_{\mathrm{c,LQG}}(\mathbf{q}) \triangleq \frac{N_{\mathrm{LQG}}(\mathbf{q})}{D_{\mathrm{LQG}}(\mathbf{q})}$. Note that (57) is feasible by construction, and it follow from Proposition 4 that its leading numerator coefficient and relative degree are the same as those of $-EG_u(\mathbf{q})$ and that its zeros are the zeros of $G_u(\mathbf{q})$ as well as n zeros at zero.

Example 2. *Feasible* $G_{\rm f}(\mathbf{q})$. Let $G_u(\mathbf{q}) = G_w(\mathbf{q}) = \frac{(\mathbf{q}-1.2)(\mathbf{q}-0.9)}{(\mathbf{q}-1.3)(\mathbf{q}^2-1.9\mathbf{q}+0.99)}$. Note that $G_u(\mathbf{q})$ is NMP and unstable. RCAC is applied with $G_{\rm f}(\mathbf{q}) = G_{\rm f,LQG}(\mathbf{q})$, $p_0 = 10$, and $n_{\rm c} = n = 3$. Figure 4(d) shows that $G_{z\tilde{u},1000}(\mathbf{q})$ and $G_{\rm f}(\mathbf{q})$ have similar frequency responses, which is consistent with the fact that $G_{\rm f,LQG}(\mathbf{q})$ is feasible. Furthermore, Figure 4(c) shows that $G_{\rm c,LQG}(\mathbf{q})$ and $G_{\rm c,1000}(\mathbf{q})$ have similar frequency responses, which suggests that RCAC converges to $G_{\rm c,LQG}(\mathbf{q})$. ◇

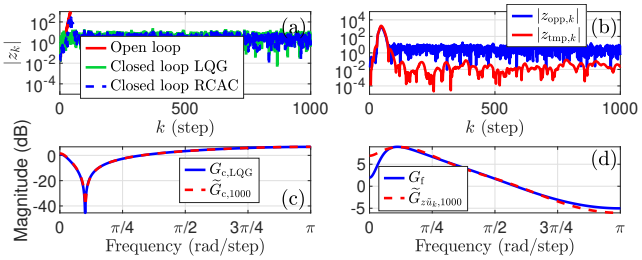

Fig. 4. Example 2: RCAC with feasible $G_{\rm f}(\mathbf{q})$.

Example 3. *Infeasible* $G_{\rm f}(\mathbf{q})$. Let

$$G_u(\mathbf{q}) = G_w(\mathbf{q}) = \frac{(\mathbf{q}-0.5)(\mathbf{q}-1.1)}{(\mathbf{q}-0.85)(\mathbf{q}^2-1.8\mathbf{q}+0.9)}. \quad (58)$$

Since $G_u(\mathbf{q})$ is NMP and asymptotically stable, Proposition 4 implies that $G_{\rm f,LQG}(\mathbf{q})$ constructed with $G_u(\mathbf{q})$ given by (58) has zeros at 0.5 and 1.1 rad/step. We construct

$$G_{\rm f,LNC}(\mathbf{q}) = \alpha_{\rm LNC} G_{\rm f,LQG}(\mathbf{q}), \quad (59)$$

$$G_{\rm f,RD}(\mathbf{q}) = \frac{1}{\mathbf{q}^{\alpha_{\rm RD}}} G_{\rm f,LQG}(\mathbf{q}), \quad (60)$$

$G_{\rm f,MP}(\mathbf{q})$, which is $G_{\rm f,LQG}(\mathbf{q})$ with its minimum phase (MP) zero at 0.5 replaced with a zero at $\alpha_{\rm MP}$ rad/step, and $G_{\rm f,NMP}(\mathbf{q})$, which is $G_{\rm f,LQG}(\mathbf{q})$ with its NMP zero at 1.1 replaced with a zero at $\alpha_{\rm NMP}$ rad/step. Note that $G_{\rm f,LNC}(\mathbf{q})$, $G_{\rm f,RD}(\mathbf{q})$, $G_{\rm f,MP}(\mathbf{q})$, and $G_{\rm f,NMP}(\mathbf{q})$, are equal to $G_{\rm f,LQG}(\mathbf{q})$, and thus feasible, for the nominal values $\alpha_{\rm LNC} = 1$, $\alpha_{\rm RD} = 0$, $\alpha_{\rm MP} = 0.5$, and $\alpha_{\rm NMP} = 1.1$, respectively. To investigate the effect of infeasibility of $G_{\rm f}(\mathbf{q})$ on RCAC, we vary $\alpha_{\rm LNC}$, $\alpha_{\rm RD}$, $\alpha_{\rm MP}$, and $\alpha_{\rm NMP}$ from their nominal values.

The *disturbance-suppression metric* $g_{\rm s}$ is defined as the ratio of the root-mean-square of the last 2000 steps of the open-loop response and the closed-loop response in dB. The case $g_{\rm s} > 0$ corresponds to disturbance suppression relative to the open loop. Simulations where either $g_{\rm s} \le 0$ or the output of the closed-loop diverges are indicated as failures.

RCAC is applied with $n_{\rm c} = n = 3$, $p_0 = 100$, and $G_{\rm f}(\mathbf{q}) = G_{\rm f,LNC}(\mathbf{q})$, $G_{\rm f}(\mathbf{q}) = G_{\rm f,RD}(\mathbf{q})$, $G_{\rm f}(\mathbf{q}) = G_{\rm f,MP}(\mathbf{q})$, and $G_{\rm f}(\mathbf{q}) = G_{\rm f,NMP}(\mathbf{q})$ for $0 \le k \le 10000$, as shown in Figure 5. In particular, Figures 5(a) and 5(e) show $g_{\rm s}$ and $\rm f_\infty$, respectively, for $G_{\rm f}(\mathbf{q}) = G_{\rm f,LNC}(\mathbf{q})$, where $\alpha_{\rm LNC} \in [-2, 8]$, which shows that infeasibility due to the sign of the leading numerator coefficient of $G_{\rm f}(\mathbf{q})$ causes failure. However, RCAC is robust to infeasibility due to the magnitude of the leading numerator coefficient of $G_{\rm f}(\mathbf{q})$. Figures 5(b) and 5(f) show $g_{\rm s}$ and $\rm f_\infty$, respectively, for $G_{\rm f}(\mathbf{q}) = G_{\rm f,RD}(\mathbf{q})$, where $\alpha_{\rm RD} \in \{0, 1, 2, 3\}$, which shows that infeasibility due to the relative degree of $G_{\rm f}(\mathbf{q})$ causes failure. Figures 5(c) and 5(g) show $g_{\rm s}$ and $\rm f_\infty$, respectively, for $G_{\rm f}(\mathbf{q}) = G_{\rm f,MP}(\mathbf{q})$, where $\alpha_{\rm MP} \in [-1.2, 1.2]$, which shows that RCAC is robust to infeasibility due to an incorrectly modeled MP zero in $G_{\rm f}(\mathbf{q})$. However, note that RCAC fails when a MP zero of $G_u(\mathbf{q})$ is replaced with a positive NMP zero in $G_{\rm f}(\mathbf{q})$. Figures 5(d) and 5(h) show $g_{\rm s}$ and $\rm f_\infty$, respectively, for $G_{\rm f}(\mathbf{q}) = G_{\rm f,NMP}(\mathbf{q})$, where $\alpha_{\rm NMP} \in [0.8, 1.5]$, which shows that RCAC is robust to infeasibility due to an incorrectly modeled NMP zero in $G_{\rm f}(\mathbf{q})$. However, note that RCAC fails when a NMP zero of $G_u(\mathbf{q})$ is replaced with a MP zero in $G_{\rm f}(\mathbf{q})$. ◇

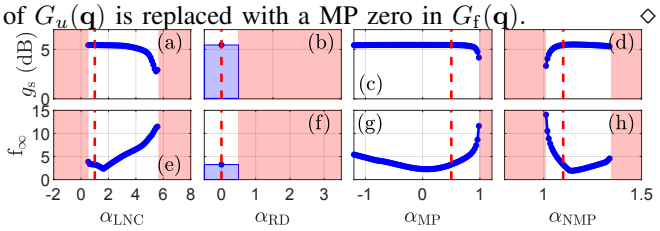

Fig. 5. Example 3: (a), (b), (c), (d), and (e), (f), (g), (h), show the disturbance suppression metric $g_{\rm s}$ and asymptotic feasibility distance $\rm f_\infty$ for $G_{\rm f}(\mathbf{q}) = G_{\rm f,LNC}(\mathbf{q})$, $G_{\rm f}(\mathbf{q}) = G_{\rm f,RD}(\mathbf{q})$, $G_{\rm f}(\mathbf{q}) = G_{\rm f,MP}(\mathbf{q})$, and $G_{\rm f}(\mathbf{q}) = G_{\rm f,NMP}(\mathbf{q})$, respectively. The vertical red dashed lines indicate the nominal values of $\alpha_{\rm LNC}$, $\alpha_{\rm RD}$, $\alpha_{\rm MP}$, and $\alpha_{\rm NMP}$.

D. Construction of $G_{\rm f}(\mathbf{q})$

Example 3 suggests that RCAC can reject disturbances with an infeasible $G_{\rm f}(\mathbf{q})$, however, $G_{\rm f}(\mathbf{q})$ must match the sign of the leading numerator coefficient and relative degree of $-EG_u(\mathbf{q})$, and include NMP zeros of $G_u(\mathbf{q})$.

Example 4. *Infeasible and Simplified* $G_{\rm f}(\mathbf{q})$. Let $G_u(\mathbf{q}) = G_w(\mathbf{q})$ be given by (58). We define the *baseline target model* $G_{\rm f,b}(\mathbf{q}) \triangleq -\frac{\mathbf{q}-1.1}{\mathbf{q}^2}$, which has the same leading numerator coefficient, relative degree, and NMP zero as $-EG_u(\mathbf{q})$. Next, we construct $G_{\rm f,LNC}(\mathbf{q}) = -\alpha_{\rm LNC}\frac{\mathbf{q}-1.1}{\mathbf{q}^2}$, $G_{\rm f,RD}(\mathbf{q}) = -\frac{\mathbf{q}-1.1}{\mathbf{q}^{2+\alpha_{\rm RD}}}$, $G_{\rm f,NMP}(\mathbf{q}) = -\frac{\mathbf{q}-\alpha_{\rm NMP}}{\mathbf{q}^2}$. Note that $G_{\rm f,LNC}(\mathbf{q})$, $G_{\rm f,RD}(\mathbf{q})$, and $G_{\rm f,NMP}(\mathbf{q})$, are equal to $G_{\rm f,b}(\mathbf{q})$, for the nominal values $\alpha_{\rm LNC} = 1$, $\alpha_{\rm RD} = 0$, and $\alpha_{\rm NMP} = 1.1$, respectively. To investigate the effect of a target model $G_{\rm f}(\mathbf{q})$ constructed using an erroneous $EG_u(\mathbf{q})$, we vary $\alpha_{\rm LNC}$, $\alpha_{\rm RD}$, $\alpha_{\rm MP}$, and $\alpha_{\rm NMP}$ from nominal.

RCAC is applied with $n_{\rm c} = n = 3$, $p_0 = 100$, and $G_{\rm f}(\mathbf{q}) = G_{\rm f,LNC}(\mathbf{q})$, $G_{\rm f}(\mathbf{q}) = G_{\rm f,RD}(\mathbf{q})$, and $G_{\rm f}(\mathbf{q}) = G_{\rm f,NMP}(\mathbf{q})$ for $0 \le k \le 10000$, as shown in Figure 6. ◇

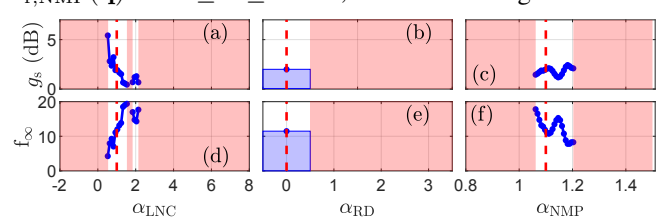

Fig. 6. Example 4: (a), (b), (c), and (d), (e), (f), show the disturbance suppression metric $g_{\rm s}$ and asymptotic feasibility distance $\rm f_\infty$ for $G_{\rm f}(\mathbf{q}) = G_{\rm f,LNC}(\mathbf{q})$, $G_{\rm f}(\mathbf{q}) = G_{\rm f,RD}(\mathbf{q})$, and $G_{\rm f}(\mathbf{q}) = G_{\rm f,NMP}(\mathbf{q})$, respectively. The vertical red dashed lines indicate the nominal values of $\alpha_{\rm LNC}$, $\alpha_{\rm RD}$, and $\alpha_{\rm NMP}$.

Example 4 suggests that $G_{\rm f}(\mathbf{q})$ can be constructed as $G_{\rm f}(\mathbf{q}) = -\alpha\frac{\prod_{i=1}^{n_{\rm z}}(\mathbf{q}-\alpha_{{\rm z},i})}{\mathbf{q}^{n_{\rm z}+r_{\rm d}}}$, where $\alpha, \alpha_{{\rm z},i}, n_{\rm z}, r_{\rm d}$, are the leading numerator coefficient, all NMP zeros, number of NMP zeros, and relative degree of $EG_u(\mathbf{q})$, respectively, and the minus sign is due to the minus sign in (1).

IV. Role of NMP Zeros in $G_{\rm f}(\mathbf{q})$

In this section we investigate the role of the retrospective performance-variable decomposition in the case where $G_{\rm f}(\mathbf{q})$ does not include NMP zeros of $EG_u(\mathbf{q})$.

Example 5. *Unmodeled NMP zeros and the retrospective performance-variable decomposition* Let $G_u(\mathbf{q}) = G_w(\mathbf{q})$ be given by (50), r_k, w_k and v_k be as in Example 1, and $G_{\rm f}(\mathbf{q}) = -\frac{1}{\mathbf{q}}$. Note that $G_{\rm f}(\mathbf{q})$ has the same leading numerator coefficient and relative degree as $-EG_u(\mathbf{q})$, however, it does not have the NMP zeros of $G_u(\mathbf{q})$. RCAC is applied with $E_z = 1$, $E_u = 0$, $E = 1$, $n_{\rm c} = 16$, and $p_0 = 10$.

As shown by Examples 1 and 2, the minimization of the retrospective performance variable extension $\hat{z}_{{\rm ext},k}(\theta_{k+1})$ leads to matching between $\widetilde{G}_{z\tilde{u},k}$ and $G_{\rm f}(\mathbf{q})$. Figure 7(h) shows that this is what happens for this example as well. Since (47) has a NMP zero at 1.1 rad/step and $G_{\rm f}(\mathbf{q})$ does not, the optimization attempts to cancel this NMP zero using the denominator of (47). This results in a controller pole at the location of the NMP zero as shown in Figure 7(g), which results in a hidden instability, as shown by the exponential divergence of u_k in Figure 7(e) and no divergence of $|z_k|$ as shown in Figure 7(a).

Additionally, the spectral radius of $D_u(\mathbf{q})D_{\rm c}(\mathbf{q}) + N_u(\mathbf{q})N_{\rm c}(\mathbf{q})$, which is the denominator polynomial of all closed-loop transfer functions, converges to a value greater than 1, which shows that all the closed-loop transfer functions are asymptotically unstable. This instability causes divergence of $z_{{\rm opp},k}(\theta_{k+1})$ and $z_{{\rm tmp},k}(\theta_{k+1})$, as shown in Figure 7(f). However, note that since $|z_k|$ and $\tilde{u}_k(\theta_{k+1})$ do not diverge, it can be seen from (26) and (30) that $\hat{z}_{{\rm ext},k}(\theta_{k+1}) \approx 0$, as shown in Figure 7(d), which implies that $z_{{\rm opp},k}(\theta_{k+1}) \approx -z_{{\rm tmp},k}(\theta_{k+1})$. ◇

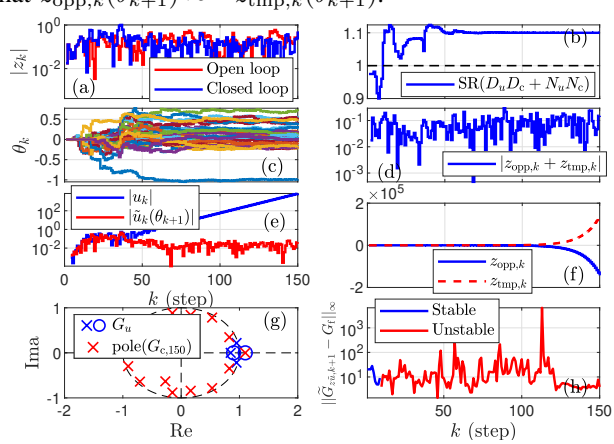

Fig. 7. Example 5: (a) open- and closed-loop responses; (b) spectral radius of $D_uD_{\rm c}+N_uN_{\rm c}$; (h) $\|\widetilde{G}_{z\tilde{u},k+1}(\mathbf{q})-G_{\rm f}(\mathbf{q})\|_\infty$, coded by color for the stability of $\widetilde{G}_{z\tilde{u},k+1}(\mathbf{q})$.

As shown in Example 5, u_k diverges exponentially in the case where $G_{\rm f}(\mathbf{q})$ does not model the NMP zeros of $EG_u(\mathbf{q})$. We investigate the ability of a nonzero E_u to weigh u_k to prevent its divergence. Note that with $E_z = 1$ and $E_u \neq 0$, using (18) and (31), it follows from (22) that

$$J_k(\theta_{k+1}) = \sum_{i=0}^{k}[\hat{z}_i^{\rm T}(\theta_{i+1})\hat{z}_i(\theta_{i+1}) + u_{i+1}^{\rm T}E_uE_u^{\rm T}u_{i+1}] + (\theta_{i+1}-\theta_0)^{\rm T}P_0^{-1}(\theta_{i+1}-\theta_0), \qquad (61)$$

where the positive semi-definite $u_{i+1}^{\rm T}E_uE_u^{\rm T}u_{i+1}$ term prevents the minimization of $\hat{z}_k(\theta_{k+1})$ through (49) in the case where u_k becomes large, thus preventing the divergence of $z_{{\rm opp},k}(\theta_{k+1})$ and $z_{{\rm tmp},k}(\theta_{k+1})$ with opposite signs. The following example demonstrates this effect.

Example 6. *Unmodeled NMP zeros and the role of E_u.* RCAC is applied with $E_z = 1$, $E_u = 2$, $E = 1$, $n_{\rm c} = 16$, and $p_0 = 10$. Figure 8(c) shows that there is no controller pole at the location of the NMP zero of $EG_u(\mathbf{q})$. Additionally, as shown in Figure 8(d), $z_{{\rm opp},k}(\theta_{k+1})$ and $z_{{\rm tmp},k}(\theta_{k+1})$ do not diverge. As a result, u_k does not diverge as shown in Figure 8(d) , and the closed-loop is stable for all $k > 153$, as shown in Figure 8(b). ◇

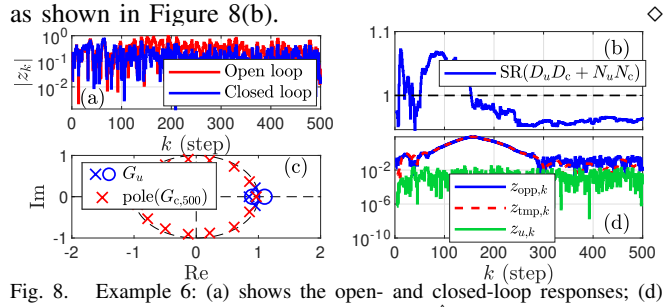

Fig. 8. Example 6: (a) shows the open- and closed-loop responses; (d) shows $z_{{\rm opp},k}(\theta_{k+1})$, $z_{{\rm tmp},k}(\theta_{k+1})$, and $z_{u,k} \triangleq u_{k+1}^{\rm T}E_uE_u^{\rm T}u_{k+1}$.

V. Conclusions

This paper showed that the retrospective performance variable can be decomposed into performance and model-matching terms, and that the optimization can result in the terms with opposite signs. However, the convergence of the controller drives the model-matching term to a small value, ensuring that the performance term is small, and thus achieving closed-loop performance.

This paper also synthesized and demonstrated numerically the essential modeling information needed to construct the target model $G_{\rm f}(\mathbf{q})$ in RCAC. Namely, the sign of the leading numerator coefficient, the relative degree, and NMP zeros of the plant $-EG_u(\mathbf{q})$. Finally, in the case where the NMP zeros of the plant were not modeled in $G_{\rm f}(\mathbf{q})$, it was shown that a nonzero control weight E_u can allow closed-loop performance.

Future research will extended the insights for essential modeling information to MIMO plants. Additionally, these insights will be used to investigate the mechanisms used by data-driven RCAC (DDRCAC) [4] – an extension of RCAC that uses concurrent identification to construct $G_{\rm f}(\mathbf{q})$ – to achieve closed-loop performance.

Funding Sources

This research was supported by ONR under BRC grant N00014-18-1-2211.

References

[1] K. F. Aljanaideh and D. S. Bernstein, "Initial Conditions in Time- and Frequency-Domain System Identification: Implications of the Shift Operator Versus the Z and Discrete Fourier Transforms," *IEEE Contr. Sys. Mag.*, vol. 38, no. 2, pp. 80–93, 2018.

[2] R. Middleton and G. Goodwin, *Digital Control and Estimation: A Unified Approach*. Prentice Hall, 1990.

[3] S. A. U. Islam and D. S. Bernstein, "Recursive least squares for real-time implementation," *IEEE Contr. Sys. Mag.*, vol. 39, no. 3, pp. 82–85, 2019.

[4] S. A. U. Islam, T. W. Nguyen, I. V. Kolmanovsky, and D. S. Bernstein, "Adaptive Control of Discrete-Time Systems with Unknown, Unstable Zero Dynamics," in *Proc. Amer. Contr. Conf.*, 2020, pp. 1387–1392.